



Full Length Article

Evaluation of the catalytic effect and migration behavior of potassium in the molten slag during the char/molten slag interfacial gasification

Xiaodan Bao, Zhongjie Shen^{*}, Haigang Zhang, Qinfeng Liang, Haifeng Liu

Shanghai Engineering Research Center of Coal Gasification, East China University of Science and Technology, P. O. Box 272, Shanghai 200237, PR China



ARTICLE INFO

Keywords:

Coal gasification
Alkali metal (K)
Molten slag
Catalytic effect
Migration behavior

ABSTRACT

The reaction of coal char particles deposited on the molten slag surface in the entrained flow gasifier was of importance to the carbon conversion and slag discharge. In this study, the catalytic effect and migration behavior of the alkali metal (K) in molten slag during the gasification reaction of char particles on the molten slag surface were investigated and evaluated by using visualization and surface analytical techniques. The results showed the ionic K in the molten slag was not deactivated and accelerated the char gasification rate and carbon conversion of char particle on the molten slag surface as a catalytic effect. The complete conversion time of char particles on the molten slag with the addition of K was reduced by about 37%–67%, compared to the time of the char gasification without molten slag or the gasification on the slag with no addition of K. The carbon conversion of char particles was increased obviously with increasing the addition of K in the molten slag. From the analyses of scanning electron microscope (SEM) and energy dispersive spectrometry (EDS), the ionic K was found to gradually migrate and accumulate to the interface between the coal char particle and molten slag during the gasification process. The migrating and accumulating amount of K to the interface increased with the increases of both carbon conversion of the char particle and K addition of the slag. With a comparative experiment of the char combustion on the slag surface, a low temperature zone below the char particle during the gasification was key to cause a migration behavior of K with other elements (e.g. Si and Al) and further acted as a catalytic effect on the gasification reaction. Finally, a mechanism of the catalytic effect and migration behavior of ionic K in the slag during the char/molten slag interfacial gasification process was uncovered in this study.

1. Introduction

The entrained flow gasification technology has been widely used to produce syngas ($\text{CO} + \text{H}_2$) as an intermediate for chemical products or fuel gas for power generation [1–3]. The operating temperature of the entrained flow gasifier is set above the ash flow temperature, with the coal ash melted and a liquid slag layer formed on the refractory wall [4]. The liquid slag layer, as a barrier to prevent the corrosion from the high-temperature molten slag [5], will protect the refractory wall and capture coal ash particles or partially-gasified char particles [6]. However, the particle deposition, which cannot be avoided in the entrained flow gasifier, subsequently affects the further conversion of solid fuels and changes the slag chemical composition, such as ash fusion, crystallization, and viscosity, etc. [7–9]. Therefore, the research on the reaction characteristics of char particles captured on the molten slag surface and their physicochemical interactions are essential and supportive to improve the conversion of coal particles and give a deep insight on char-

to-slag behavior during the entrain flow gasification process.

Generally, the results of solid particles impacting onto the wall in the gas–solid reactor include adhesion and rebound, which are affected by the degree of the particle conversion, particle size, impact velocity, surface tension of molten slag or particle, and slag viscosity, etc. [10–12]. The conversion degree of a coal particle affected the physical and chemical properties of the particle surface, such as the porous structure, elemental distribution and composition, etc. [12–14]. Li et al. [10] found that the surface of a char particle with a high carbon conversion rate was sticky and this particle was easy to be captured by the wall of the reactor during the entrained flow gasification process. The sticky surface of a partially-reacted particle was caused by the melting of the coal ash to slag with a low melting point, which was originally attributed to the high contents of alkali and alkaline earth metals (AAEMs) in the coal ash sample, and this further resulted in a stronger deposition tendency [15,16]. In addition, Naruse et al. [11] found that the deposition amount of coal ash particles on the pipe surface increased

^{*} Corresponding author.

E-mail address: zjshen@ecust.edu.cn (Z. Shen).

<https://doi.org/10.1016/j.fuel.2021.121881>

Received 11 June 2021; Received in revised form 13 August 2021; Accepted 28 August 2021

Available online 3 September 2021

0016-2361/© 2021 Elsevier Ltd. All rights reserved.

with the decrease of the ash melting temperature. A submodel considering the effects of the viscosity, surface tension, impacting angle, and particle velocity on the particle deposition of the wall in the slagging system was proposed by Ni et al. [12], and the results showed that large molten slag particles had a higher deposition probability than small particles. Moreover, the deposition probability was proved to increase with the impact velocity and droplet temperature while the effect of the contact angle was weak. Differently, for the deposition process of low-temperature coal ashes from a study by Luan et al. [15], the large particle size and high impact velocity significantly inhibited the deposition of particles. Troiano et al. [17–18] studied the segregation and deposition behaviors of particles toward the wall and found that the particle segregation behavior resulted into a dense-dispersed particle phase established on the liquid slag layer. This established dense-dispersed phase was proved to be beneficial to the gasification performance, together with the increased particle residence time and promoted carbon conversion. Thus, the interaction between the char particle and molten slag layer was key to the conversion and slag properties on the wall of an entrained flow gasifier.

It was found that there were three regimes (entrapped carbon regime, segregated carbon regime – incomplete char-coverage, and segregated carbon regime – extensive carbon-coverage) after the interaction between carbon particles and slag wall [19–20]. The first regime was that char particles deposited and immersed inside the slag wall, which could not further react with the near-wall gas and finally transformed into the residual carbon in the slag layer [21]. The residual carbon in the slag would react with SiO_2 and Fe_2O_3 to form SiC , CO , FeO , or Fe_3C as carbothermal reaction [22]. However, the increase of the graphitization degree of the residual char was found to be not conducive to the occurrence of carbothermal reaction [8]. Wang et al. [23,24] found that the increase of the Fe_2O_3 content in the coal ash increased the occurrence temperature, degree, and reaction rate of the carbothermal reaction, while the $\text{SiO}_2/\text{Al}_2\text{O}_3$ ratio of the coal ash mainly affected the carbothermal reaction of Si and C. The second and third regimes were that some deposited particles on the slag surface, not fully embedded in the slag layer due to buoyancy or interfacial tension, continued to react with the near-wall gas. These particles were predicted and validated to occupy about 20 wt% of the total injected particles in the entrained flow gasifier from a study by Xu et al. [25]. Li et al. [26–27] found that the molten slag accelerated the carbon conversion and intrinsic surface reaction rate with the increasing addition amount of the slag into the coal. The residual carbon in the coarse slag contained more active sites and could promote the gasification reaction [28]. Otherwise, the molten slag was proved to be beneficial for the gasification of char particles on the slag surface, with more heat absorbed from the slag and particle temperature increased [29]. Zhang et al. [30] found that the morphological change of the molten slag was the main factor to affect the gasification reactivity of coal char particles. When the gasification temperature was below the coal ash fusion temperature, the solid ash layer covered part of the char particle surface and resisted the diffusion of the reactant gas to the reaction surface. The solid ash layer transformed to a liquid layer when the temperature was above the melting temperature, enhancing the heat transfer and improving the gasification reaction rate.

Coal ash particles that contained high contents of alkali and alkaline earth metals (AAEMs) (e.g. Na and K) were easy to be melted and deposited on the wall, resulting in the formation of the liquid slag layer [31–32]. Then, the liquid slag layer with high contents of AAEMs further intensified the particle deposition behaviors of both coal ash/slag particles and un-reacted char particles [33]. AAEMs can reduce the ash fusion temperatures [34] and improve the slag flow ability, while also have a catalytic effect on the gasification reaction [35–36]. It was found that K_2CO_3 had a strong catalytic effect on the steam gasification of ash-free char particles [37]. Alkali metals accelerated the gasification rate by changing the structure and reaction path inside the char particle [38–39]. Among these AAEMs, the catalytic ability of K was better than Na and Ca [40], while Si and Al in the coal ash could react with K at high

temperature to form alkali aluminosilicates [41]. The catalytic ability of K was considered to be deactivated and difficult to recover from coal ash residues [42]. When the Si/Al ratio in the coal mineral increased, more silicate aluminates containing K formed and inhibited the gasification reaction [43]. Song et al. [44] found that the K-bearing salt migrating to the coal char existed in the form of insoluble sulfate, and the reaction temperature and Al/Si ratio of coal minerals were key to the redistribution of potassium during gasification. However, Liu et al. [45] found that the gasification rate of petroleum coke particles on the surface of the slag with adding K inside was promoted, showing bulk of pores on the particle surface. This catalytic effect of K on the petroleum coke gasification was contacted with the abovementioned results of ash-free coals in Ref. [37]. However, the action mechanism of AAEMs in the molten slag, such as K, during the gasification process of coal char on the molten slag surface is still unclear.

In this study, the effect of alkali metal (K) in the molten slag on the gasification reaction of char particles on the molten slag surface was investigated by using visualization and surface analytical techniques. The comparative experiments were carried out, including the gasification of char particles without molten surface and the char combustion on the slag surface. The complete reaction time and carbon conversion were measured and calculated to evaluate the catalytic effect of K in the molten slag on the char gasification. The effect of a different amount of K addition in the molten slag on the char gasification was studied. The morphology evolution of the char particle and element distribution on the char-slag interface during the gasification process were analyzed by using scanning electron microscopy (SEM) coupled with energy dispersive spectrometry (EDS). Additionally, the migration behavior of K on the interface of char particle and slag surface at different carbon conversions was studied. Finally, a mechanism of the catalytic effect and migration behavior of ionic K in the slag during the char/molten slag interfacial gasification process was uncovered in this study.

2. Experimental

2.1. Materials

In this study, the coal char sample was prepared from a Chinese bituminous coal (Shenfu Coal) in a drop tube furnace at 1350°C under an argon atmosphere. The gas flow rate of Ar was set to 1.2 L/min and the feeding rate of the raw coal sample was 200 g/h. The proximate and ultimate analyses of the raw coal and coal char samples are tested and the results are given in Table 1. The particle size of the coal char is chosen to 150 μm . Generally, the average particle size of the pulverized coal used in the entrained flow gasifier is below 100 μm . There is a part of coal particles of which the particle size is larger than 100 μm . In addition, during the fast pyrolysis of the coal in the entrained flow gasifier, the fragmentation and swelling behaviors of coal particles occurred and the particle size would increase [46]. Besides, larger particles cost longer conversion time, which would be easier to deposit on

Table 1

The proximate and ultimate analyses of coal and coal char samples used in this study (air-dried basis).

Samples	Raw coal	Coal char
Proximate analysis (wt%)		
Moisture	7.68	3.45
Ash	7.64	10.22
Volatile matter	26.70	3.21
Fixed carbon	57.98	83.12
Ultimate analysis (wt%)		
Carbon	78.36	84.52
Hydrogen	3.37	1.01
Nitrogen	1.12	1.05
Sulfur	0.77	0.28
Oxygen	8.74	2.92

the slag layer. Therefore, the particle size of the coal char sample used in this study exceeds 100 μm .

The coal ash sample was prepared in a N17/HR-K muffle furnace (Nabertherm Company, Lilienthal, Germany) at 815 $^{\circ}\text{C}$ in the air atmosphere. To study the effect of K in the slag on the char gasification, a different amount of K_2CO_3 (5.0 wt%, 10.0 wt%, and 15.0 wt%) was added to the coal ash sample. The addition amount of K_2CO_3 was set based on the weight of the coal ash. Four different coal ashes with adding K_2CO_3 from 0.0 wt% to 15.0 wt% are named S-0 K, S-5 K, S-10 K and S-15 K, respectively. Then, these four different coal ashes were pre-melted in a high-temperature furnace (Shanghai Yifeng Electric Furnace Co., Ltd, China) at 1350 $^{\circ}\text{C}$ for 1 h, to fully mix K_2CO_3 with coal ash. During the heating process of the pre-melting experiment, part of K_2CO_3 began to decompose into K_2O and CO_2 or volatilized to the ambient environment [47], which caused K loss in the slag sample. Therefore, the actual amount of K in the mixed sample was lower than the theoretical value calculated. The actual chemical compositions of pre-melted coal ashes were given in Table 2. The chemical compositions of coal ash samples were detected by Advant'X IntellipowerTM 3600 X-ray fluorescence (XRF, Thermo Fisher Scientific, America).

2.2. Experimental methods

The experiment of the char gasification on the molten slag surface was carried out on a visual experimental platform, with combing a high-temperature hot stage and a high-resolution microscope. The detailed information of the experimental platform is shown in Fig. 1. Before each experiment, the temperature controller is calibrated by gradually heating a small piece of silver wire to a high temperature and comparing the displayed temperature on the system with the silver melting point. The temperature measurement part of this system is calibrated and repeated twice or three times to keep the measuring error below 0.5 %.

About 0.5 mg coal ash sample was put on a sapphire wafer (99.9% purity of Al_2O_3) and char particles with an average particle size of 150 μm were spread on the coal ash layer. The sapphire wafer with the coal ash layer and char particles was put in the crucible of the high-temperature hot stage. The space of the crucible was sealed with a hot stage lid and a gas flow of N_2 (0.3 L/min, 99.999% purity) was injected to remove the air in the chamber of the hot stage. Then, the coal ash and char particles were heated to 300 $^{\circ}\text{C}$ at the heating rate of 50 $^{\circ}\text{C}/\text{min}$ and held for 1 min to remove moisture. Afterwards, the crucible and samples were heated to 1300 $^{\circ}\text{C}$ at the heating rate of 100 $^{\circ}\text{C}/\text{min}$ and held for 5 min to achieve a quasi-static energy balance. Next, the N_2 flow was switched to CO_2 flow (0.1 L/min, 99% purity) for the gasification reaction. Meantime, the digital camera of the microscope started to record the gasification process of char particles as a video. The comparative experiments were carried out in this study, including the char gasification without slag and the combustion of char particles on the molten slag surface. The experiment of the char gasification without the molten slag surface was to compare the effect of the slag with/without adding K inside on the char gasification. The experiment of the char combustion

Table 2

Chemical compositions (wt.%) of coal ash and coal slag samples before and after pre-melting experiments.

Sample	Before pre-melting experiment				After pre-melting experiment		
	S-0 K	S-5 K	S-10 K	S-15 K	S-5 K	S-10 K	S-15 K
SiO_2	46.18	44.66	43.23	41.89	45.23	44.02	42.51
Al_2O_3	19.04	18.41	17.82	17.27	19.28	18.06	17.35
Fe_2O_3	11.01	10.65	10.31	9.99	10.02	9.92	10.34
CaO	17.79	17.2	16.65	16.14	16.89	16.39	16.12
K_2O	1.35	4.6	7.64	10.49	4.35	7.47	9.77
TiO_2	0.72	0.7	0.67	0.65	0.67	0.67	0.66
MgO	1.54	1.49	1.44	1.4	1.25	1.31	1.18
Na_2O	1.94	1.88	1.82	1.76	1.95	1.9	1.85
SO_3	0.43	0.41	0.42	0.41	0.36	0.26	0.22

on the molten slag surface was to study the effect of the temperature change on the interface of char and molten slag on the element migration. The recorded video was converted to picture format. To study the migration behavior of K during the gasification process, the partially-gasified char sample on the molten slag surface was prepared by injecting gas within different time. The carbon conversion of the partially-gasified sample was calculated and determined corresponding to the shrinkage of the cross-sectional area. In this study, capital C, S, and K are used to represent the char sample, coal slag and K_2CO_3 . For instance, C-S-0 K represents the experimental sample with char particle and slag sample but no addition of K. C-S-5 K represents the experimental sample with char particle and slag with the addition of 5 wt% K_2CO_3 inside.

ImageJ software [48] was used to measure the cross-sectional area of char particles during the gasification process. The ash content of the coal char sample was about 10.22 wt%. During the char gasification on the molten slag surface, coal ash was melted into the liquid slag. The ash content in the coal char particle was ignored. It was assumed that that char particles are isotropic spherical particles with a constant density. Based on the measurement of the cross-sectional area, the particle diameter at time t can be expressed as

$$d_t = 2\sqrt{\frac{A_t}{\pi}} \quad (1)$$

where d_t is the particle diameter at time t, μm , and A_t is the measured cross-sectional area of a char particle at time t, μm^2 . With the ignored ash content in the particle, char particles showed shrinking characteristics during the reaction process, and the carbon conversion of the char particle can be calculated as follows:

$$x = 1 - \frac{m_t}{m_0} = 1 - \frac{\rho V_t^3}{\rho V_0^3} \quad (2)$$

Where x is the carbon conversion, m_t and m_0 are particle masses at time t and initial time, respectively. ρ is the char particle density, kg/m^3 , V_t and V_0 are particle volumes at time t and initial time, m^3 , respectively. Thus,

$$x = 1 - \frac{d_t^3}{d_0^3} = 1 - \left(\frac{A_t}{A_0}\right)^{\frac{3}{2}} \quad (3)$$

where d_0 is the particle diameter at initial time, μm , and A_0 is the measured cross-sectional area of char particles at initial time, μm^2 .

After the experiment on the visual experimental platform, the coal slag, char particle, and partially-gasified char particle samples on the sapphire wafer were analyzed by using scanning electronic microscope (SEM) for micro morphologies. Moreover, the element distribution on the slag surface and the interface between the char particle and molten slag was tested via both point scanning and elemental mapping of energy dispersive spectrometer (EDS). The interface between the char particle and molten slag was scanned via SEM-EDS by removing the partially-gasified char particle.

3. Results and discussion

3.1. Coal char gasification process

Fig. 2 shows the photographs of the gasification processes of char particles with and without molten slag of adding K inside at the temperature of 1300 $^{\circ}\text{C}$. During the gasification process, the shape evolution of a coal char particle acted as a shrinking particle. With the molten slag and the increasing addition of K, the complete reaction time of the char particle decreased. The complete reaction time of the char particle without the molten slag was 14.0 s, as shown in Fig. 2a. In Fig. 2b, the reaction time on the molten slag with no addition of K decreased to 9.0 s. The molten slag promoted the gasification rate and reduced the conversion time of char particles, which has been proved in our previous

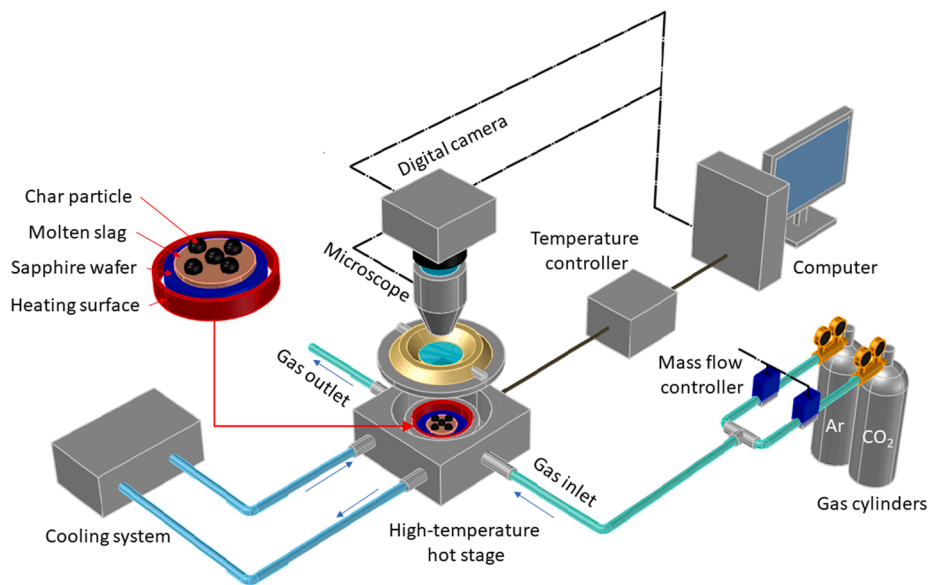


Fig. 1. The schematic drawing of the visual experimental platform.

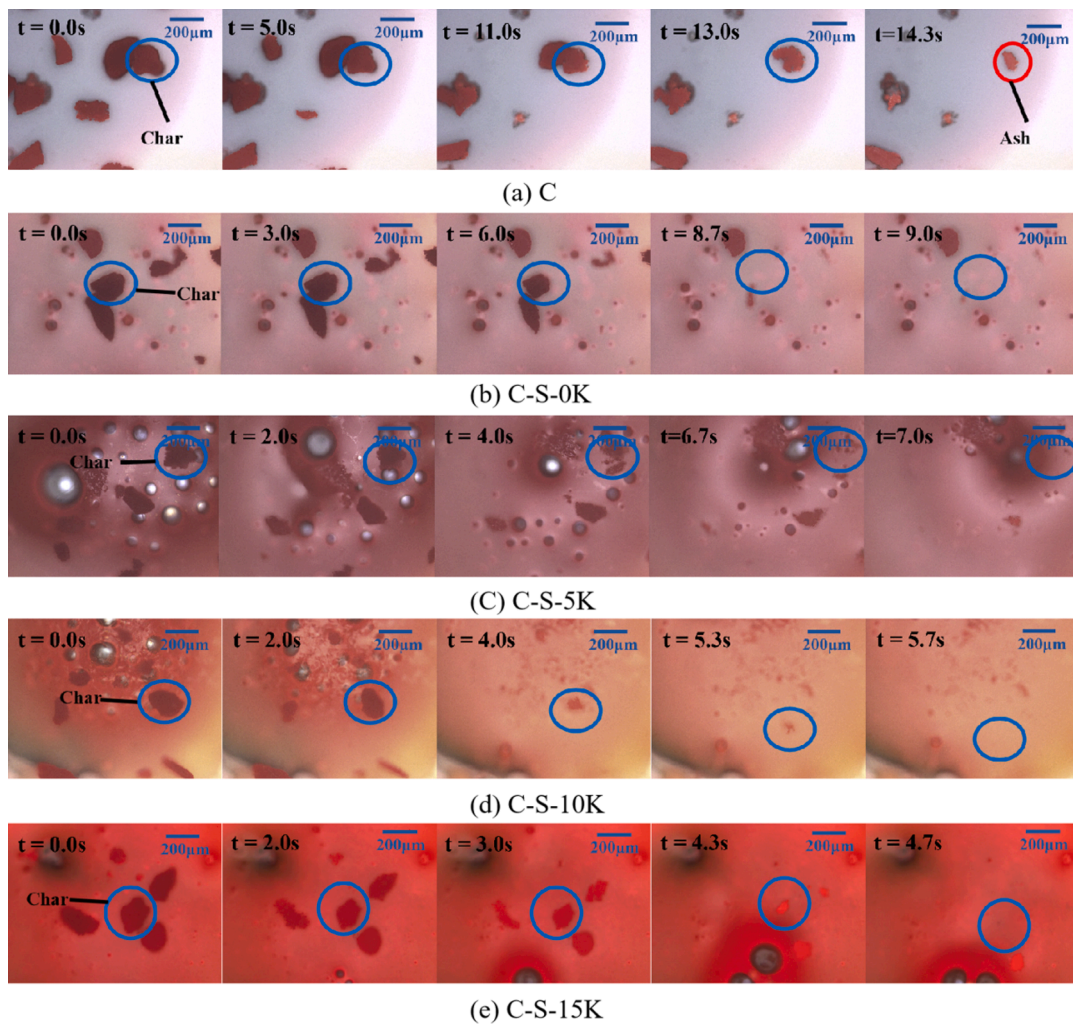


Fig. 2. Photographs of the gasification processes of char particles with or without molten slag and addition of K at 1300 °C. t in this figure only denotes the reaction time.

studies [29]. When adding 5.0 wt% K_2CO_3 to the slag, the complete reaction time of char particles on the molten slag surface was reduced to 7.0 s, as shown in Fig. 2c. Furthermore, the Complete reaction time of char particles in Fig. 2d and 2e decreased to 5.7 s and 4.7 s, respectively, corresponding to the molten slags with adding 10.0 and 15.0 wt% K_2CO_3 . Additionally, bubbles were found to form on the interface of char and slag surface when the slag was added K_2CO_3 inside. The formation of bubbles during the gasification of char particles on the slag surface contained CO [49], and this indicated the enhanced activity of char gasification on the molten slag surface. Due to the different time when each char particle contacted with the reactant gas, the initial reaction time of each particle was different in the furnace. Thus, from the images shown in Fig. 2a, the time of each char particle started to shrink or react was different. The time difference in Fig. 2a was because larger particles cost more time to complete the gasification reaction. Therefore, the initial reaction time is different for each char particle. However, regardless of the contacting time, the complete reaction time of char particles was similar under the same experimental condition.

3.2. Carbon conversion of char particles

The evolutions of the cross-sectional area and carbon conversion of coal char particles with or without molten slag surface and adding K inside at 1300 °C are given in Fig. 3. The cross-sectional area of a char particle changed a little in the N_2 atmosphere. When CO_2 was injected to the furnace, CO_2 reacted with char particles, as shown in Fig. 3a. Therefore, t denotes the gas transportation time of both N_2 and CO_2 in Fig. 3a and t' denotes the reaction time in Fig. 3b. The evolution of cross-sectional area of the char gasification showing the black cube line in Fig. 3 acted as a “slowly-rapidly-slowly” decreasing tendency. In the middle and late stages of the reaction, the cross-sectional area decreased slowly, which was different from other four lines belonged to the char gasification on the molten slag of adding K. With the increasing addition of K in the slag, the shrinkage rate of the cross-sectional area was rapid, indicating more carbon reacted with CO_2 on the molten slag surface. The results calculated from Eq. (3) showed that higher carbon conversion was found for the char particles on the molten slag with adding K, compared to the char particle and chars on the molten slag without adding K. The molten slag with adding K could improve the carbon conversion of char particles during the gasification on the molten slag surface, especially after the conversion of 0.7.

The averaged complete reaction time of char particles with error bars are measured and given in Fig. 4. The averaged complete reaction time of char particles means the average value of the complete reaction time of each char particle under the same reaction condition. The bar graph clearly shows that the molten slag with adding K could reduce the total reaction of char particles and promote the gasification.

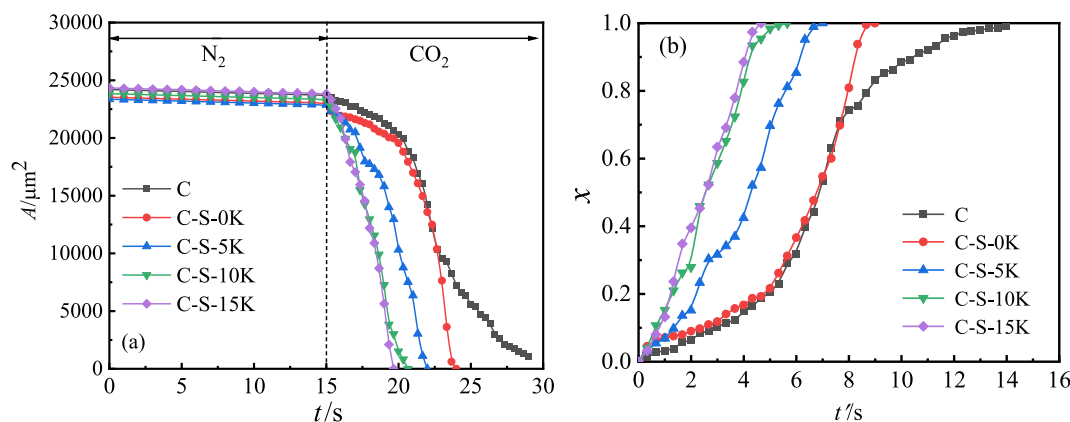


Fig. 3. Evolutions of the cross-sectional area (a) and carbon conversion (b) of char particles under different reaction conditions. t denotes the gas transportation time of both N_2 and CO_2 in Fig. 3a and t' denotes the reaction time in Fig. 3b.

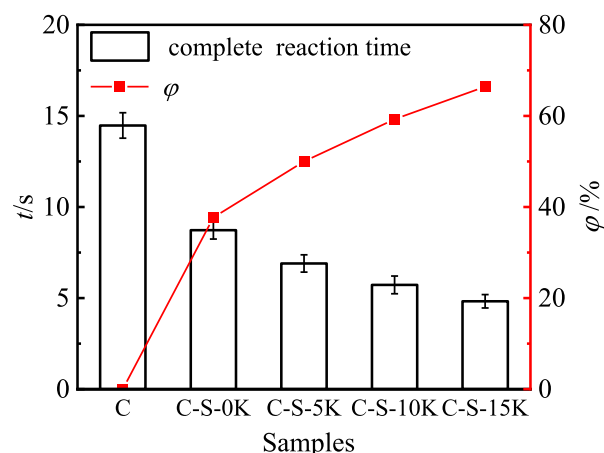


Fig. 4. Complete reaction time and reduced time ratio of char particles with the relationship of adding a different amount of K in the coal slag at 1300°C.

A reduced time ratio ϕ of coal char particles was calculated and used to characterize the promotion of the addition of K in the slag for the char gasification in this study. The complete reaction time of the char particle without slag or adding K is denoted as t'_1 from the result of the experiment. t'_1 was 14.3 s as shown in Fig. 2a. Then, the reduced time ratio (ϕ) can be expressed as

$$\phi = \frac{t'_1 - t'}{t'_1} \times 100\% \quad (4)$$

where ϕ is the reduced time ratio for the gasification of coal char particles, and t' is the complete reaction time of coal char particles on the surface of slag mixed with different content of K, s.

The initial time of the gasification reaction was measured from the evolution of the cross-sectional area of each char particle, and it was determined when this particle started to shrink that the cross-sectional area reduced as shown in Fig. 3. The cross-sectional area of a char particle changed a little in the N_2 atmosphere. When CO_2 was injected to the furnace, char particles reacted with CO_2 and their cross-sectional area started to shrink, as shown in Fig. 3a. For the gasification without molten slag, the stop point of the reaction time was determined when the cross-sectional particle stopped to change. However, during the char gasification on molten slag surface, due to the melting behavior of the coal ash into the slag, the stop point of the reaction time was determined when the particle was missing on the slag surface. The melting behavior of the coal ash and the gasification reaction of the coal char were carried out simultaneously on the molten slag surface. The

complete reaction time of char particles on the molten slag without adding K was reduced by about 40% compared to char particles without molten slag. With adding K_2CO_3 from 5.0 wt% to 15.0 wt% in the slag, the reduced time ratio φ increased from 37% to 67%. The gasification of char particles absorbed heat from the molten slag. In addition, the complete reaction time of char particles on the molten slag surface decreased with the increasing K content. It can be inferred that K in the molten slag has catalytic effect on char particles gasification.

3.3. Morphology and element distribution

The SEM images of char particles on the molten slag surface were captured and the element distribution was scanned by using mapping function of EDS. The results of the particle morphology and element distribution at different carbon conversion on the molten slag surface, of which the slag sample was added 5.0 wt% K_2CO_3 , are given in Fig. 5. Basically, all elements were uniformly distributed on the molten slag surface, showing in Fig. 5a, when there was no reaction of the char particle. When the carbon conversion was 0, the aimed elements (e.g. K, Si, Al, Ca, Fe, C, Na, and Mg) were tested and distributed uniformly

around the char particle on the surface, which is displayed in Fig. 5b. When the char particle started to react with CO_2 on the slag surface, it was found that K accumulated to the interface of this particle while other elements, such as Si, Al, Ca, Fe, Mg, and Na, were accumulated on the slag surface out of the particle zone. At carbon conversion of 38% in Fig. 5d, K was obviously found on the particle interfacial zone with less Si and Al, but Ca, Fe, Mg, and Na were not accumulating to this zone. When the carbon conversion of char particle on the molten slag surface was about 70% (Fig. 5e), EDS analytical results showed a strong intensity of K distribution on the interface of char particle and molten slag. Besides, weaker intensities of Si and Al were also found than K, but other elements, including Ca, Fe, Mg, and Na, were still showing no signal in this zone. When the conversion of a char particle is approaching 99%, owing to less gasification reaction on the slag surface, the heat transfer between the char particle and surrounding slag and the temperature difference was reduced. Then, the temperature gradient force became smaller on the interface of slag and char particle, and less K migrated to the interface with Al and Si. In addition, the temperature of the slag was held at $1300^\circ C$, which was higher than the flow temperature of the coal ash. Therefore, all elements were uniformly distributed in the slag, as

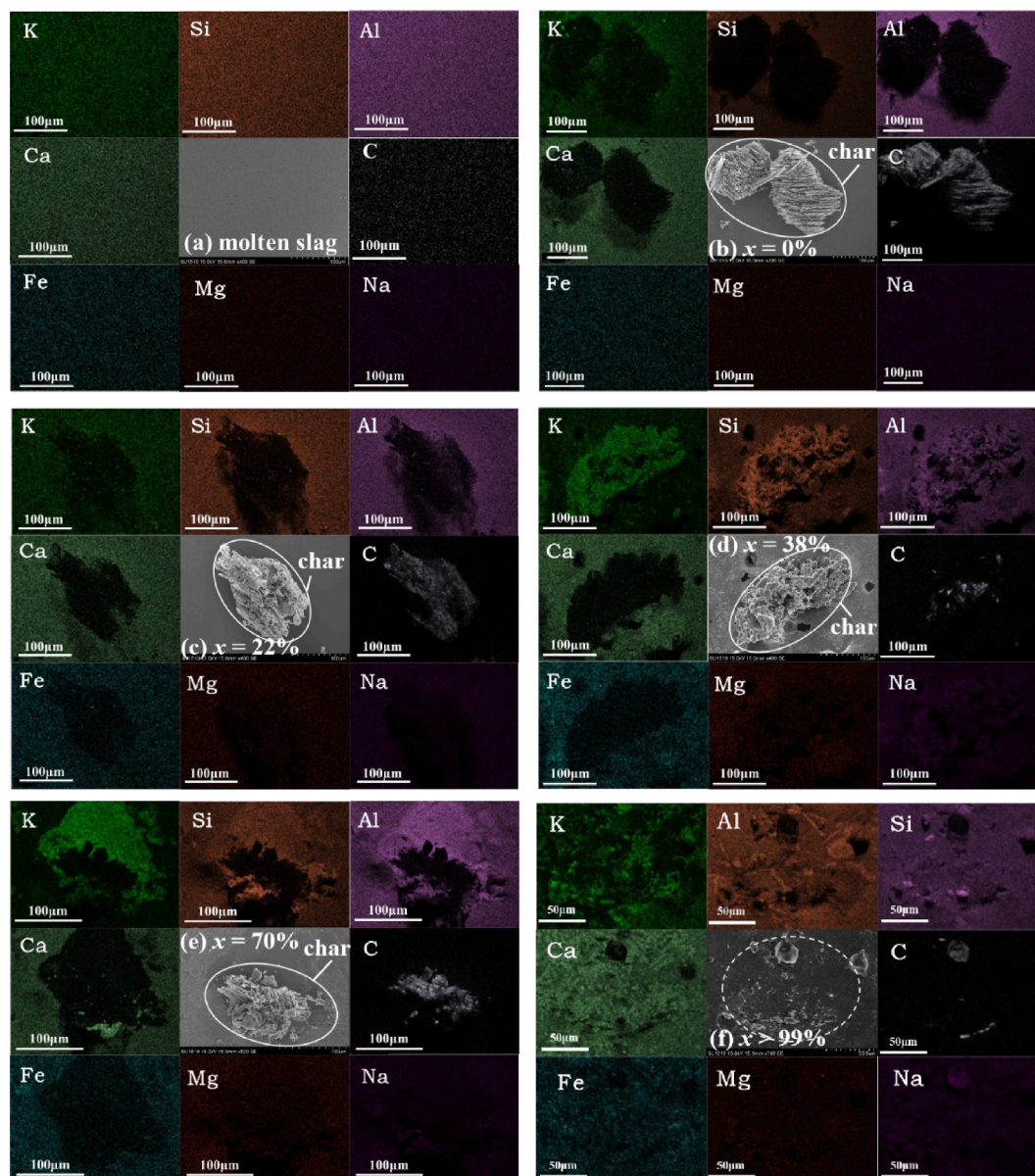


Fig. 5. SEM images and element distribution of char particles on the molten slag surface with the addition of 5 wt% K_2CO_3 at different carbon conversion.

shown in Fig. 5f. From Fig. 5, the results indicated that K accumulated to the interface of char particle and molten slag, and this accumulation increased with the consumption of carbon during the gasification process. Besides, Si and Al followed K and showed an accumulation behavior around the particle as well.

The element distribution around the char particle during the gasification was tested in Fig. 5. To study the migration behavior of the elements during the char gasification on the molten slag surface, the average content of the element on the slag surface out of the particle zone, defined as w_1 , and the average content of the element on the char-slag interface, defined as w_2 , were tested and compared with error bars. The partially-gasified char particle above the slag layer was removed for the distribution test of the element on the interface. The element composition on the interface between the partially-gasified char particles and the molten slag added 5 wt% K_2CO_3 were correspondingly analyzed by SEM-EDS, and the results are given in Fig. 6. Results showed that the content of Al on the interface was closed to the value on the slag surface while it accumulated at the conversion of 38%. At the early stage of the gasification reaction ($x < 38\%$), Si was mainly distributed in the slag, showing from the negative value of the difference between w_1 and w_2 . Then, Si migrated to the interface between the char particle and slag with the positive value of $w_2 - w_1$, and this can be validated from the elemental mapping results in Fig. 5d and e. The difference of the K content between w_2 and w_1 increased with the carbon conversion, indicating that K migrated to the interface and accumulated on the interface between the char particle and molten slag during the char gasification process. However, the content of other alkali metal and alkali earth metals (e.g. Ca, Na, and Mg) and Fe decreased and displayed negative values ($w_2 - w_1$) when the carbon conversion increased. Therefore, the results showed that the K element in the slag had a stronger migration behavior than other elements during the char gasification on the molten surface.

3.4. Effect of K_2CO_3 addition

In addition, the element distribution of the char-slag interface with the effect of K_2CO_3 addition in the coal ash was investigated in this study. The SEM images and element compositions on the interface of the

char particle and molten slag surface are exhibited in Fig. 7. Char particles on the molten slag surface in the left column of Fig. 7 were partially-gasified particles at the carbon conversion around 40%, and then were removed for the interface between char particle and slag as shown in the middle column of Fig. 7. In Fig. 7, elements on spots 1 and 2 were tested from the slag surface not on the interface, and elements on spots 3 and 4 were from the interface between the char particle and molten slag. The results showed that the contents of Na and Mg on the slag surface (spots 1 and 2) were similar to the contents on the interface (spots 3 and 4), when the slag sample had no K_2CO_3 addition or addition of 5 wt% K_2CO_3 . However, when the addition of K_2CO_3 in the coal ash exceeded 5.0 wt%, the contents of Na and Mg on the interface (spots 3 and 4 in Fig. 7c and 7d) decreased. The content of Al on the interface (spots 3 and 4 in Fig. 7a and 7b) was higher than the value on the slag surface (spots 1 and 2 in Fig. 7a and 7b) when the addition of K_2CO_3 was below 5.0 wt%. When the coal ash was added a high adding amount of K_2CO_3 , Al was uniformly distributed on both slag surface and char-slag interface (all tested spots in Fig. 7c and 7d). However, the contents of Ca and Fe on the slag surface (all spots 1 and 2 in Fig. 7) were higher than the value on the interface (all spots 3 and 4 in Fig. 7), indicating that Ca and Fe would migrate to the slag surface out of the char particle zone.

Comparing the content of K with other elements on the surface, both K contents on the slag surface (w_1) and the interface between the char particle and slag (w_2) increased with the adding amount of K_2CO_3 in the slag, and the results are given in Fig. 8. Besides, the difference of w_1 and w_2 showed an increasing linear relationship with the adding amount of K_2CO_3 (below 10.0 wt%), which means that the migration amount of K also increased with the addition of K_2CO_3 in the slag. When the adding amount was about 15.0 wt%, the content of K on the interface (C-S-15 K) was similar to the condition of C-S-10 K. This was attributed to the increasing content of K of the slag and the difference between these two interfaces decreased accordingly.

3.5. Theoretical analysis and mechanism

The char gasification is an endothermic reaction and hence the temperature of the char particle will decrease during the gasification process without extra heat support. The molten slag has been proved to

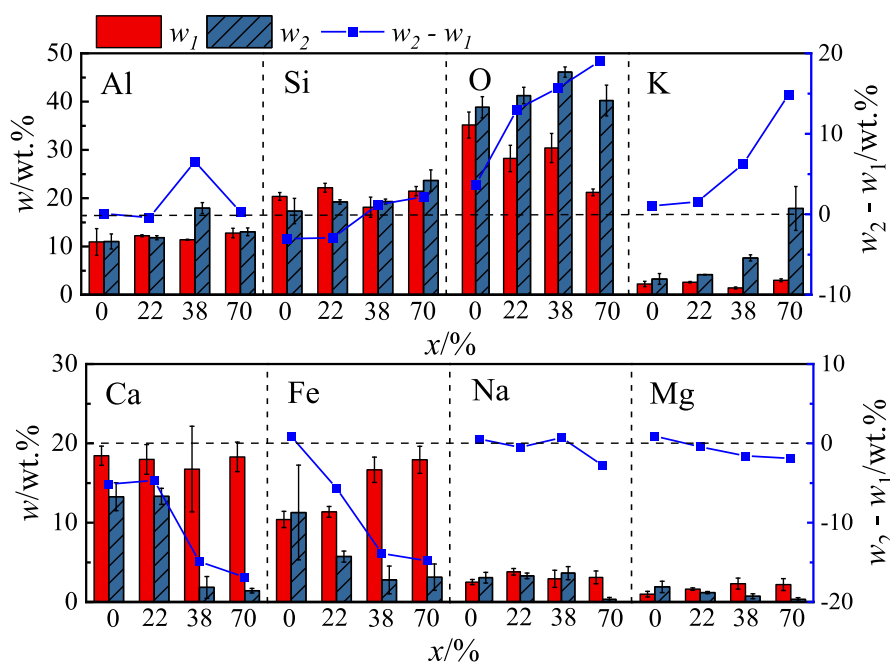


Fig. 6. Average contents (w/wt.%) of tested elements on the molten slag surface (w_1) and the interface between char particle and slag (w_2) and their difference values corresponding to different carbon conversions. The slag sample was added 5.0 wt% of K_2CO_3 before pre-melting experiment.

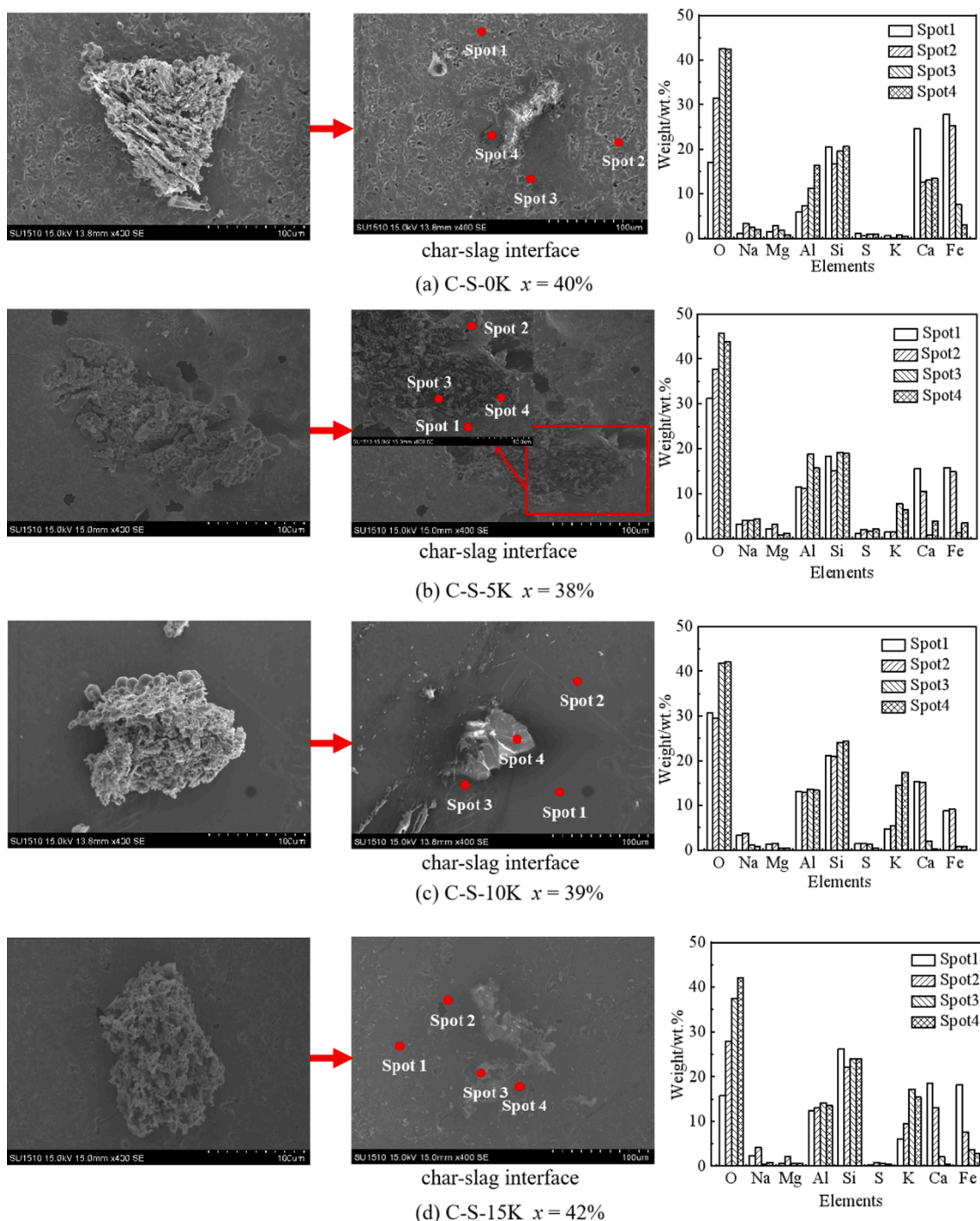


Fig. 7. SEM images and element compositions on the interface of char particle and molten slag with adding a different amount of K_2CO_3 . Spots 1 and 2 are on the slag surface while spots 3 and 4 are on the interface of char particle and molten slag.

benefit for the char gasification on its surface in the previous studies [29]. This promotion of the char gasification on the molten slag surface can be considered as a “hot bath” effect from the slag. From this study, results also showed that K would migrate to the interface between the char particle and slag and further act as a catalytic effect on the gasification. Similar results were proved by the studies of Liu et al. [45] on the gasification of the petroleum coke on the slag surface. This catalytic effect was validated based on the comparison of the reduced gasification time of char particles on the slag surface with and without adding K_2CO_3 . Because the gasification reaction of char particles absorbed heat from the molten slag, the temperature on the interfaces would be lower

than the surrounding slag and a low-temperature zone was formed on this interface. A low-temperature zone was speculated to be related to the migration of K, and with the increasing carbon conversion, this further caused the further catalytic effect on the gasification on the molten slag surface.

To uncover the mechanism of K migration from the slag to the char-slag interface, a comparative experiment of the char combustion on the molten slag surface was carried out in this study. The slag sample for the combustion experiment was added 5.0 wt% K_2CO_3 inside and same with the gasification experiment. Similarly, the element distribution on the partially-combusted char particle and slag was analyzed via SEM-EDS.

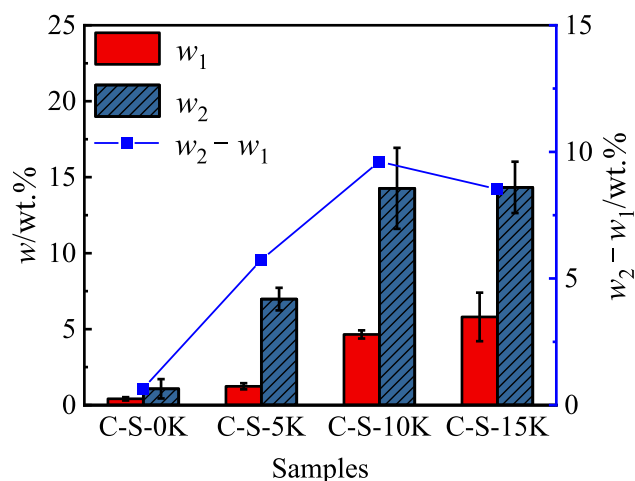


Fig. 8. The content (w/wt.%) of K element analyzed by EDS on the slag surface (w_1) and interface of char particle and slag (w_2) with adding a different amount of K_2CO_3 .

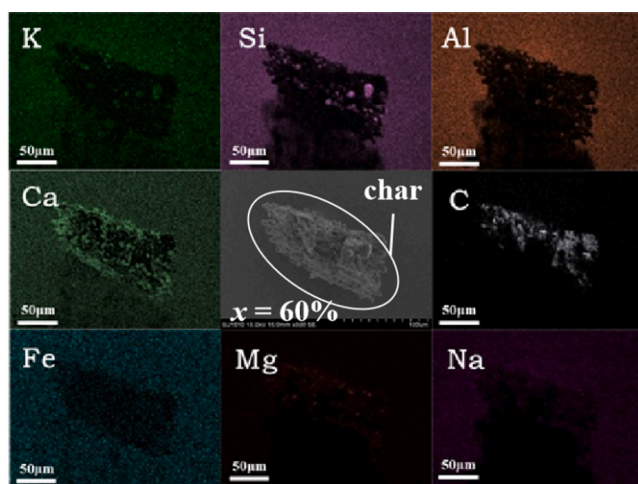


Fig. 9. Elemental distribution analysis of char particle and slag with char conversion of 60% and slag mixed with 5.0 wt% K_2CO_3 .

The elemental mapping results are given in Fig. 9. It was clear that lower intensities of K, Si, and Al content distribution were found on the zone of the partially-combusted char particle. In addition, except for Ca, intensities of Fe, Na, and Mg content distribution were similar to the distribution of K, Si, and Al elements. Ca showed an opposite result to other elements, owing to the high content of Ca in the coal ash. The comparative experimental results pointed out that K had no migration during exothermic combustion reactions. The zone where the char particle was located in was marked in a circle. The difference inside or outside of the circle for the distribution of Si, K, and Al was caused by the migration behavior during the interfacial combustion reaction of char particles on the molten slag surface. The zone below the char particle contained small amounts of Si, K, and Al, which may be due to different temperature distribution on the slag surface and these elements (Si, Al, and K) migrated to this zone. The dark zone out of the circle for Si and Al distributions was due to the high temperature that forced these elements to migrate to the slag zone, of which the results were opposite to the gasification reaction. However, the elements (Ca, C, and Fe) on the interface between the char particle and slag were found on the image.

Nevertheless, the low-temperature zone on the interface between the char particle and slag might cause the elemental migration behavior even if this temperature gradient was small. It was proved by Shen et al.

[50] that K and Na had strong migration behaviors during the crystallization process. K migrated into the amorphous phase while Mg, Fe, and Na showed different migration behaviors. Due to the exothermic behavior of the crystallization, K migrated to the amorphous phase zone of relatively lower temperature, which was similar to the results found in this study. One common point was that K and Na both migrated to the slag surface, and in the melts with high basicity, alkali metals diffused rapidly and commonly against concentration gradients, which changed the concentration across entire ionic coupling diffusions [51]. Owing to the low content of Na in the coal ash of this study, the migration of Na was not found but K showed a strong migration behavior. K and Na were found to have coupled diffusion properties in the melts, belonging to fast-diffusing components, and were also proved to have a strong coupling with slow diffusing components, such as Al and Si. [52]. From the results in Fig. 5d and 5e, Si and Al both had strong intensities similarly with K on the interface of char particle and slag.

From the results in Figs. 6 and 7, main elements on the interface between the char particles and slag were Si, Al, K and O, and their stoichiometric ratio was about 2:1:1:6, when the conversion was 70% for the char particle on the slag mixed with 5.0 wt% K_2CO_3 and 39% for the char particle on the slag mixed with 10.0 wt% K_2CO_3 . It can be inferred that the mineral herein was close to potassium silicate aluminate ($KAlSi_2O_6$), which was formed on the interface due to the low-temperature zone. K was also proved to migrate to the crystal surface during crystallization [50]. The schematic drawing of the mechanism of the migration behavior of K in the molten slag and its catalytic effect on the char gasification was proposed and shown in Fig. 10. Therefore, it can be concluded that K would migrate to the interface of char and slag surface with the low-temperature zone occurred during the gasification on the molten slag surface. Due to the weak thermal absorption of char particles at the initial stage of reaction, the temperature difference between the char particle and its surrounding slag was small, and meantime the migration behavior of K was not significant. With the carbon consumption, more heat was absorbed from the slag. A low-temperature zone was formed between the char particle and its surrounding slag. This low-temperature zone provided a driving force to lead a K accumulation on the interface and further caused a catalytic effect on the char gasification. Al and Si elements, as coupling elements in the slag melts, migrated with K and formed crystals on the interface.

4. Conclusion

An investigation of the evaluation of the catalytic effect and migration behavior of potassium in the molten slag on the gasification reaction of char particles on the molten slag surface was conducted in this study. K at ionic state was not deactivated in the molten slag and still had catalytic effect on the char gasification. Compared to the char gasification and the char gasification on the slag without adding K, char particles on the slag surface with extra addition of K had less reaction time, and the complete reaction time can be reduced from 37% to 67%, achieving a higher carbon conversion. The increasing amount of K in the molten slag also strengthened the catalytic effect on the char gasification. With the morphological and elemental distribution analyses, the ionic K in the slag melt had a strong migration behavior during the char gasification process on the molten slag surface. K was found to migrate and accumulate around the gasifying char particle, and this migrating and accumulating amount increased with the carbon conversion. On the interface between the char particle and slag, Si and Al were found to accumulate with coupling the K migration. A mechanism of the migration behavior and catalytic effect of potassium in the molten slag during the char gasification on the molten slag surface was uncovered. The low-temperature zone caused by the char gasification on the interface between the char particle and slag gave a driving force to the migration and accumulation of K in the slag melt, which further had a catalytic effect and promotion on the gasification.

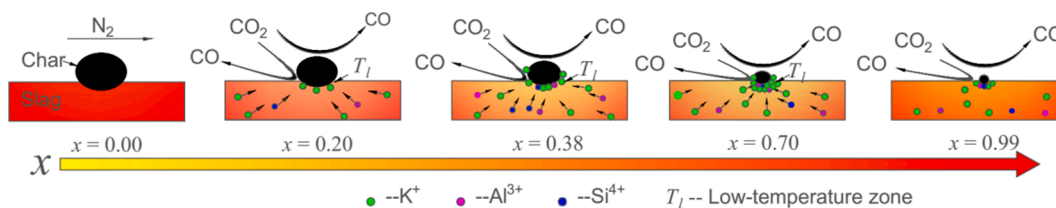


Fig. 10. The schematic drawing of the migration mechanism of K in slag and its catalytic effect on the char gasification on the molten slag surface.

CRediT authorship contribution statement

Xiaodan Bao: Resources, Data curation, Formal analysis, Investigation, Methodology, Software, Visualization, Writing - original draft, Writing - review & editing. **Zhongjie Shen:** Conceptualization, Supervision, Formal analysis, Methodology, Software, Writing - original draft, Writing - review & editing, Project administration, Funding acquisition. **Haigang Zhang:** Resources, Data curation, Formal analysis, Investigation. **Qinfeng Liang:** Conceptualization, Validation, Resources, Investigation, Methodology, Writing - review & editing. **Haifeng Liu:** Conceptualization, Supervision, Validation, Formal analysis, Methodology.

Declaration of Competing Interest

The authors declare that they have no known competing financial interests or personal relationships that could have appeared to influence the work reported in this paper.

Acknowledgements

This study was supported by the National Natural Science Foundation of China (Grant No. 21908063).

References

- Ryzhkov A, Bogatova T, Gordeev S. Technological solutions for an advanced IGCC plant. *Fuel* 2018;214:63–72.
- Gong X, Lu W, Guo X, Dai Z, Liang Q, Liu H, et al. Pilot-scale comparison investigation of different entrained-flow gasification technologies and prediction on industrial-scale gasification performance. *Fuel* 2014;129:37–44.
- Higman C, Tam S. Advances in coal gasification, hydrogenation, and gas treating for the production of chemicals and fuels. *Chem Rev* 2014;114(3):1673–708.
- Krishnamoorthy V, Pisupati S. A critical review of mineral matter related issues during gasification of coal in fixed, fluidized, and entrained flow gasifiers. *Energies* 2015;8(9):10430–63.
- Stickler DB, Gannon RE. Slag-coated wall structure technology for entrained flow gasifiers. *Fuel Process Technol* 1983;7(3):225–38.
- Xue Z, Guo Q, Gong Y, Wu X, Wang F, Yu G. Detailed deposition characteristics around burner plane in an impinging entrained-flow coal gasifier. *Chem Eng Sci* 2019;198:85–97.
- Chen D-X, Tang L-H, Zhou Y-M, Wang W-M, Wu Y-Q, Zhu Z-B. Effect of char on the melting characteristics of coal ash. *J Fuel Chem Technol* 2007;35(2):136–40.
- Wang J, Kong L, Bai J, Li H, Bai Z, Li X, et al. The role of residual char on ash flow behavior, Part 1: The effect of graphitization degree of residual char on ash fusibility. *Fuel* 2018;234:1173–80.
- Kong L, Bai J, Li W, Wen X, Liu X, Li X, et al. The internal and external factor on coal ash slag viscosity at high temperatures, Part 2: Effect of residual carbon on slag viscosity. *Fuel* 2015;158:976–82.
- Li S, Wu Y, Whitty KJ. Ash deposition behavior during char-slag transition under Simulated Gasification Conditions. *Energy Fuels* 2010;24(3):1868–76.
- Naruse I, Kamihashira D, Miyauchi Y, Kato Y, Yamashita T, Tominaga H. Fundamental ash deposition characteristics in pulverized coal reaction under high temperature conditions. *Fuel* 2005;84(4):405–10.
- Ni J, Yu G, Guo Q, Zhou Z, Wang F. Submodel for predicting slag deposition formation in slagging gasification systems. *Energy Fuels* 2011;25(3):1004–9.
- Dai P, Dennis JS, Scott SA. Using an experimentally-determined model of the evolution of pore structure for the gasification of chars by CO₂. *Fuel* 2016;171:29–43.
- Zhou Z, Shen Z, Liang Q, Liu H. Sub-particle scale study on the melting behavior of Zhundong coal ash based on the heterogeneous distribution of elements. *Combust Flame* 2020;216:223–31.
- Luan C, You C, Zhang D. An experimental investigation into the characteristics and deposition mechanism of high-viscosity coal ash. *Fuel* 2014;119:14–20.
- Akiyama K, Pak H, Tada T, Ueki Y, Yoshiie R, Naruse I. Ash deposition behavior of upgraded brown coal and bituminous coal. *Energy Fuels* 2010;24(8):4138–43.
- Troiano M, Montagnaro F, Solimene R, Salatino P. Modelling entrained-flow slagging gasification of solid fuels with near-wall particle segregation. *Chem Eng J* 2019;377:119962. <https://doi.org/10.1016/j.cej.2018.09.123>.
- Troiano M, Solimene R, Montagnaro F, Salatino P. Char/ash deposition and near-wall segregation in slagging entrained-flow gasification of solid fuels: from experiments to closure equations. *Fuel* 2020;264:116864. <https://doi.org/10.1016/j.fuel.2019.116864>.
- Montagnaro F, Salatino P. Analysis of char-slag interaction and near-wall particle segregation in entrained-flow gasification of coal. *Combust Flame* 2010;157(5):874–83.
- Montagnaro F, Brachi P, Salatino P. Char-wall interaction and properties of slag waste in entrained-flow gasification of coal. *Energy Fuels* 2011;25(8):3671–7.
- Wu S, Huang S, Ji L, Wu Y, Gao J. Structure characteristics and gasification activity of residual carbon from entrained-flow coal gasification slag. *Fuel* 2014;122:67–75.
- Liu H, Luo C, Toyota M, Kato S, Uemiyama S, Kojima T, et al. Mineral reaction and morphology change during gasification of coal in CO₂ at elevated temperatures. *Fuel* 2003;82(5):523–30.
- Wang Ji, Kong L, Bai J, Zhao H, Xue K, Zhu X, et al. The role of residual char on ash flow behavior, Part 3: Effect of Fe₂O₃ content on ash fusibility and carbothermal reaction. *Fuel* 2020;280:118705. <https://doi.org/10.1016/j.fuel.2020.118705>.
- Wang Ji, Kong L, Bai J, Zhao H, Guhl S, Li H, et al. The role of residual char on ash flow behavior, Part 2: Effect of SiO₂/Al₂O₃ on ash fusibility and carbothermal reaction. *Fuel* 2019;255:115846. <https://doi.org/10.1016/j.fuel.2019.115846>.
- Xu J, Liang Q, Dai Z, Liu H. Comprehensive model with time limited wall reaction for entrained flow. *Fuel* 2016;184:118–27.
- Li P, Yu Q, Qin Q, Lei W. Kinetics of CO₂/coal gasification in molten blast furnace slag. *Ind Eng Chem Res* 2012;51(49):15872–83.
- Li P, Yu Q, Xie H, Qin Q, Wang K. CO₂ gasification rate analysis of datong coal using slag granules as heat carrier for heat recovery from blast furnace slag by using a chemical reaction. *Energy Fuels* 2013;27(8):4810–7.
- Wu T, Gong M, Lester Ed, Wang F, Zhou Z, Yu Z. Characterisation of residual carbon from entrained-bed coal water slurry gasifiers. *Fuel* 2007;86(7–8):972–82.
- Shen Z, Liang Q, Xu J, Zhang B, Liu H. In-situ experimental study of CO₂ gasification of char particles on molten slag surface. *Fuel* 2015;160:560–7.
- ZHANG L-M, WANG J-F, BAI Y-H, SU W-G, SONG X-D, YU G-S. In-situ study of Ningdong char particles gasification characteristics on the interface of ash layer and slag. *J Fuel Chem Technol* 2020;48(2):129–36.
- Wei Bo, Tan H, Wang X, Ruan R, Hu Z, Wang Y. Investigation on ash deposition characteristics during Zhundong coal combustion. *J Energy Inst* 2018;91(1):33–42.
- Li G, Wang C, Wang P, Du Y, Liu X, Chen W, et al. Ash deposition and alkali metal migration during Zhundong high-alkali coal gasification. *Energy Procedia* 2017;105:1350–5.
- Yong SZ, Gazzino M, Ghoniem A. Modeling the slag layer in solid fuel gasification and combustion-Formulation and sensitivity analysis. *Fuel* 2012;92(1):162–70.
- Wang Y, Xiang Yu, Wang D, Dong C, Yang Y, Xiao X, et al. Effect of sodium oxides in ash composition on ash fusibility. *Energy Fuels* 2016. <https://doi.org/10.1021/acs.energyfuels.5b02722>.
- Lin X, Li C, He X, Dai J, Xu D, Wang Y. Study on the mechanism of calcium catalyzed CO₂ gasification of lignite. *Fuel Process Technol* 2021;213:106689. <https://doi.org/10.1016/j.fuproc.2020.106689>.
- Islam S, Kopycinski J, Liew SC, Hill JM. Impact of K₂CO₃ catalyst loading on the CO₂-gasification of Geneses raw coal and low-ash product. *Powder Technol* 2016;290:141–7.
- Wu X, Tang J, Wang J. A new active site/intermediate kinetic model for K₂CO₃-catalyzed steam gasification of ash-free coal char. *Fuel* 2016;165:59–67.
- Guo S, Jiang Y, Liu T, Zhao J, Huang J, Fang Y. Investigations on interactions between sodium species and coal char by thermogravimetric analysis surface. *Fuel* 2018;214:561–8.
- Zhu H, Wang X, Wang F, Yu G. In Situ Study on K₂CO₃-Catalyzed CO₂ Gasification of Coal Char: Interactions and Char Structure Evolution. *Energy Fuels* 2018;32(2):1320–7.
- Li Y, Yang H, Hu J, Wang X, Chen H. Effect of catalysts on the reactivity and structure evolution of char in petroleum coke steam gasification. *Fuel* 2014;117:1174–80.
- Formella K, Leonhardt P, Sulimma A, van Heek K-H, Jüntgen H. Interaction of mineral matter in coal with potassium during gasification. *Fuel* 1986;65(10):1470–2.
- Bruno G, Buroni M, Carvani L, Piero GD, Passoni G. Water-insoluble compounds formed by reaction between potassium and mineral matter in catalytic coal gasification. *Fuel* 1988;67(1):67–72.

- [43] Masnadi MS, Grace JR, Bi XT, Lim CJ, Ellis N, Li YH, et al. From coal towards renewables: catalytic/synergistic effects during steam co-gasification of switchgrass and coal in a pilot-scale bubbling fluidized bed. *Renew Energy* 2015; 83:918–30.
- [44] Song Y-C, Li Q-T, Li F-Z, Wang L-S, Hu C-C, Feng J, et al. Pathway of biomass-potassium migration in co-gasification of coal and biomass. *Fuel* 2019;239:365–72.
- [45] Liu M, Shen Z, Liang Q, Xu J, Liu H. In situ experimental study of CO₂ gasification of petcoke particles on molten slag surface at high temperature. *Fuel* 2021;285: 119158. <https://doi.org/10.1016/j.fuel.2020.119158>.
- [46] Shurtz RC, Kolste KK, Fletcher TH. Coal Swelling Model for High Heating Rate Pyrolysis Applications Randy C. *Energy Fuels* 2011;25(5):2163–73.
- [47] Lehman RL, Gentry JS, Glumac NG. Thermal stability of potassium carbonate near its melting point Lehman. *Thermochim Acta* 1998;316(1):1–9.
- [48] National Institutes of Health. ImageJ software. <https://imagej.nih.gov/ij/>.
- [49] Shen Z, Liang Q, Xu J, Liu H. In situ study on the formation mechanism of bubbles during the reaction of captured chars on molten slag surface. *Int J Heat Mass Transf* 2016;95:517–24.
- [50] Shen Z, Hua X, Liang Q, Xu J, Han D, Liu H. Reaction, crystallization and element migration in coal slag melt during isothermal molten process. *Fuel* 2017;191: 221–9.
- [51] Watson EB. Basalt contamination by continental crust: some experiments and models. *Contrib Mineral Petr* 1982;80(1):73–87.
- [52] Acosta-Vigil A, London D, Morgan GB. Chemical diffusion of major components in granitic liquids: implications for the rates of homogenization of crustal melts. *Lithos* 2012;153:308–23.